The Hurst Exponent as an Indicator of the Behaviour of a Model Monopile in an Ocean Wave Testing Basin

Vikram Pakrashi[1,2], Richard O'Shea[1,2], Vesna Jaksic[1,2] and Jimmy Murphy[2]

[1]Dynamical Systems and Risk Laboratory, Civil and Environmental Engineering, School of Engineering, University College Cork, Ireland

[2]Beaufort, Environmental Research Institute, School of Engineering, University College Cork, Ireland

v.pakrashi@ucc.ie

Abstract. With the importance of renewable energy well-established worldwide, and targets of such energy quantified in many cases, there exists a considerable interest in the assessment of wind and wave devices. While the individual components of these devices are often relatively well understood and the aspects of energy generation well researched, there seems to be a gap in the understanding of these devices as a whole and especially in the field of their dynamic responses under operational conditions. The mathematical modelling and estimation of their dynamic responses are more evolved but research directed towards testing of these devices still requires significant attention. Model-free indicators of the dynamic responses of these devices are important since it reflects the as-deployed behaviour of the devices when the exposure conditions are scaled reasonably correctly, along with the structural dimensions. This paper demonstrates how the Hurst exponent of the dynamic responses of a monopile exposed to different exposure conditions in an ocean wave basin can be used as a model-free indicator of various responses. The scaled model is exposed to Froude scaled waves and tested under different exposure conditions. The analysis and interpretation is carried out in a model-free and output-only environment, with only some preliminary ideas regarding the input of the system. The analysis indicates how the Hurst exponent can be an interesting descriptor to compare and contrast various scenarios of dynamic response conditions.

1. Introduction

Popularity of offshore wind and wave energy devices is growing steadily with time [1,2] and such devices are increasingly being considered in deeper waters [3]. While the offshore devices are getting popular and their co-location in high wind and wave [4] conditions ideally leads to a more efficient generation of energy from these natural resources, it also creates problems related to monitoring for maintenance and management since there is limited access to these structures. While relatively calm periods of 'weather-windows' may be employed for operations and maintenance [5] of these devices, continuous online monitoring is preferable for reasons of accessibility, safety and quality of data.

Monitoring of such devices pose a challenge since the devices are most appropriately tested only under deployed condition and not enough deployment has taken place globally to understand the full-scale dynamic behavior of these structures. Consequently, the developed models of the devices have some uncertainty or error associated to them. On the other hand, forces from wind and wave are difficult to measure for these devices to accessibility, cost and logistics issues. While efficient

monitoring of these devices are important and instrumented structures have become more commonplace in different fields of engineering [6,7,8], the uncertainty in models and the non-availability or poor quality of input force data for these structures lead towards development of performance indicators of monitoring indicators that are dependent of their dynamic responses under operational conditions. This output-only approach has significant potential to be used and a number of applications have recently illustrated this [9,10]. In this regard, applications in the field of offshore renewables have been scarce. This paper presents the Hurst exponent of the dynamic responses of such structures as a possible output-only indicator for their monitoring. In this connection, several tests have been carried out on a model monopile structure. The paper is expected to illustrate how Hurst exponents can be important for monitoring these offshore wind and wave renewable energy devices and also highlight the importance of developing and using output-only markers of monitoring in this field.

2. Experimental Setup

2.1. Description of the scaled monopile model

The Froude scaled [11] model monopile device was tested as a model of a point absorber mounted on a mono pile support which was free to move in heave. While some of the details of the model may be accessed from [11], this section briefly reports the setup for the ease of understanding and for completeness. The monopile consisted of an inner steel frame of square tubing of 30mm outside dimension and 3mm thickness. The inner steel frame was bolted to a base comprised of four metal legs. This was then attached to a large circular gravity base which sat on the bottom of the wave basin during testing. A plastic pipe, 110mm outside diameter, 3mm thickness and 2688mm in length was then attached to the steel frame. The plastic pipe was attached to the inner steel frame at four points along the pipe where load cells were mounted and was also attached to the base of the frame. Two air columns or pipes were contained within the plastic tubing. These air columns or pipes were constructed from plastic tubing 25mm outside diameter and 1.5mm thickness. At one end of the pipes were pistons which were subsequently attached to the point absorber during testing to compress the air in the pipes. At the other end of each pipe was an orifice which could be varied in diameter in order to adjust the damping of the motion of the point absorber when attached to the pistons. These orifices were initially situated above the surface of the water but were moved to a subsurface position during testing.

The point absorber was a buoyant cylinder, 380mm outside diameter with a 120mm bore, which was able to move in heave (vertically) against the mono pile. The point absorber was connected to the pistons during testing. The mass of the point absorber was varied by the addition of strips of lead to the outer rim of the point absorber. The entire model was placed in a wave basin with a constant water depth of 1m for testing. Figure 1 presents the photograph of the wave basin where the tests were carried out along with the photo of the model monopile.

Figure 1. Photographs of ocean wave testing basin and model monopile.

2.2. Instrumentation during testing of the scaled monopile model

Readings (in N) were obtained from four load cells located at different heights of the scaled monopile model. The measured force was the force that was exerted between the inner steel frame of the

monopile and the outer plastic tubing (sewage pipe) of it. The load cells were attached to the inner metal frame using two bolts and were attached to the outer casing using one bolt. The nomenclature of load cells and the heights of different bolts are presented in Table 1. Table 2 outlines the exposure conditions of the difference load sensors during testing.

Table 1. Setting Word's margins for A4 and US Letter paper.

Load Cell Name	Height of bottom-most bolt above the tank bottom (mm)	Height of top-most bolt above the tank bottom
Yellow	333	433
Green	651	751
Red	971	1071
Brown	1171	1271

Table 2. Exposure conditions of load cells during testing.

Load cell	Conditions
Yellow	Constantly submerged
Green	Constantly submerged
Red	Submerged and above water at all wave amplitudes.
Brown	Constantly above water

The red load cell is alternately submerged and exposed to air for all the wave heights. Figure 2a provides the indicative locations of load cells and Figure 2b annotates the various parts of the model.

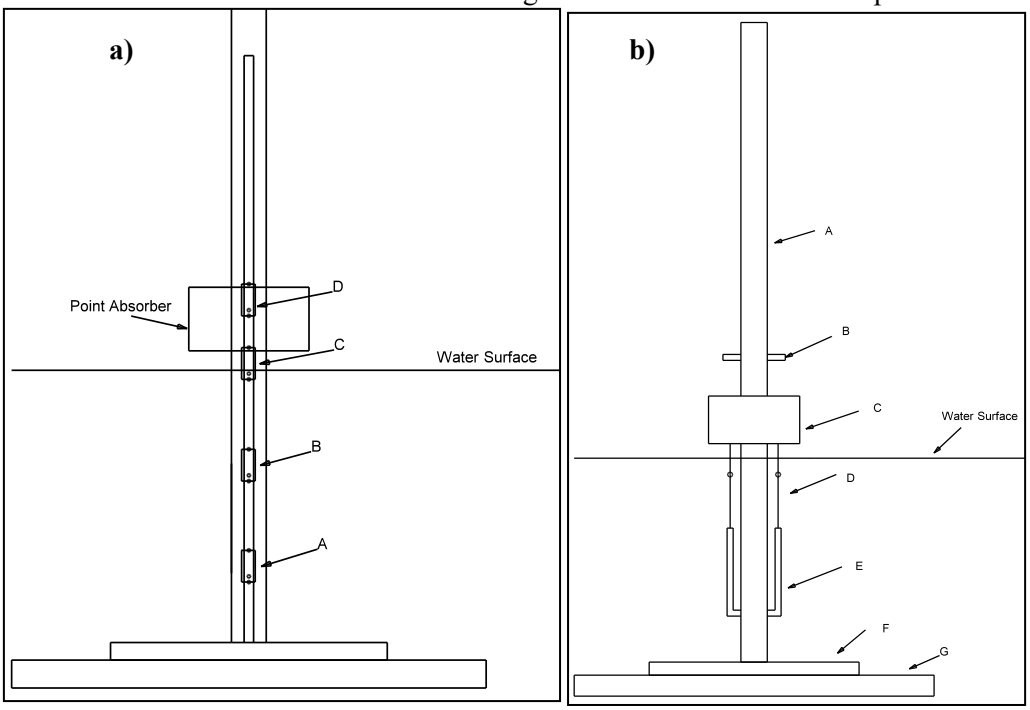

Figure 2. a) P Load Cell Location. A: Yellow, B: Green, C: Red, D: Brown. b) A: Mono pile, B: Orifice, C: Point Absorber, D: Connecting Rods, E: Pistons, F: Frame Base, G: Gravity Base

Each load cell was offset by a given amount so as to be able to distinguish them from one another during testing. Before each new configuration of each setup, a still water reading of all sensors was obtained. The average still water reading of each load cell during testing is presented in Table 3. In

order to determine the actual readings from the subsequent tests, the average value of the still water readings were subtracted from the experimentally obtained readings in terms of their magnitude.

Table 3. Still-water readings corresponding to various load cells.

Load Cell	Average Still Water Reading (including offset) (N)
Yellow	0
Green	-10
Red	-20
Brown	-30

Two water level probes were situated on either side of the point absorber and monopile assembly measuring the height of the water surface (mm) during testing. Two pressure sensors, one at the top of each piston, were used in the testing of the monopile and point absorber measuring the pressure in the pistons (mmH_2O) during the tests. Adjustments related to still water readings were carried out as presented in this section.

2.3. Details of experiments

Five different configurations of experiments were carried out in the wave basin. These differing set ups were designed to determine the effect of; wave amplitude, wave period, point absorber mass, the resistance to motion of the pistons and the effect of damping on the model.

*2.3.1. Set-up 1.*This consisted of the mono pile alone without the point absorber attached. The mono pile was placed in the wave basin and was exposed to Froude scaled waves of 60, 90 and 120 mm height. The period of the waves were varied for all different wave amplitudes. Additionally, the monopile was subject to wave samples using the Bretschneider wave spectrum in order to simulate a more realistic set of sea condition.

2.3.2. Set-up 2. This test configuration consisted of the mono pile and the point absorber which was free to move in heave against the mono pile. The point absorber was not attached to the pistons in order to eliminate the effect of the piston friction on the movement of the point absorber. Tests conducted here involved varying the mass of the point absorber and the period of the waves while keeping the amplitude of the waves constant.

2.3.3. Set-up 3. Tests conducted involved attaching the pistons to the point absorber and varying the period of the waves for constant wave amplitude of 60mm. There was no damping of the point absorber motion as the damping ratio was set to 1. The damping ratio is the ratio of the orifice to the diameter of the piston. A damping ratio of 1 implies that the piston is essentially open at one end. The effect of damping on the motion on the point absorber is absent in this set-up and only the effect of the piston friction is investigated in this set-up.

2.3.4. Set-up 4. Testing consisted of fixing the value of the mass of the point absorber to 6.1kg, attaching the pistons to the point absorber and varying the damping ratio to values of 100, 44 and 400. Each configuration was exposed to waves of amplitude 60mm and varying period. The purpose of this set-up was to determine the effect of damping on the mono pile and the point absorber. During set-up 4 the orifice was exposed to air, i.e. it was above the surface of the water.

2.3.5. Set-up 5. The model was changed more significantly in set up 5. The orifice was moved to an underwater position in order to increase the damping on the motion of the point absorber and to better model the effect of a load on the point absorber. The first third of tests carried out involved varying the mass of the point absorber between 6.1kg and 10.1kg, while it was connected to the

pistons, with a constant damping ratio of 100 and was exposed to waves of varying periods and constant amplitude of 60mm.Following this, the damping was removed (DR =1). In this configuration, the mass of the point absorber was varied between 6.1kg and 10.1kg, DR was kept constant at 1 and the model was exposed to waves of constant amplitude (60mm) and varying period. The final portion of testing carried out consisted of varying the mass of the point absorber between 6.1kg and 10.1kg while maintaining a set damping ratio of 400 and exposing the device to waves of constant amplitude (60mm) and varying period.

3. Output-Only Analysis and Hurst Exponents

This section outlines the idea behind Hurst exponent for completeness and discusses some advantages related to using this marker for monitoring. Details of this approach can be found in various literature [12, 13] and applications for infrastructure elements have recently been considered [14].

The q-order moments of the distribution of the increments of a time series y(t) obtained from the monitoring of an offshore renewable energy device with a value at t^{th} time instant with t=ν, 2ν,...kν,...T is considered, where T is the time period of observation, ν is the time resolution of observation and k is an arbitrary positive integer value. The stochastic evolution of the series is characterised and related to the generalised Hurst exponent H(q) through

$$K_q(\tau) = \frac{\left\langle | y_j(t+\tau) - y_j(t) |^q \right\rangle}{\left\langle | y_j(t) |^q \right\rangle} \sim \left(\tau / \nu\right)^{qH(q)} \quad (1)$$

The slope of the graph of qH(q) against q was used to estimate the Hurst exponent.A Hurst exponent based approach is extremely useful when a wide range of underlying activities exist within a system over a measured length of time, but the measurement from the system is not suitable for Fourier analysis based or time-frequency analysis based [15, 16] methods. The method can be quite useful for monitoring offshore renewable energy devices since an approximate model or only the output responses can be used to obtain Hurst exponent as a marker for such monitoring.

4. Results

Around 150 tests were carried out for the five set-up conditions described in a previous section in this paper and the Hurst exponents were estimated. The different values of estimated Hurst exponents at different load cells are presented in Figure 3. The horizontal axis represents the index of the test carried out, while the vertical axis represents the estimated Hurst exponent. The scatter of the exponents is quite similar, with the Yellow load cell, submerged deepest in water, showing a larger scatter. Table 4 summarises the value of the estimated Hurst exponents for different cells excluding the stillwater readings and the submerged load cells seem to distinguish themselves from those which are not. The estimated Hurst exponents seem to increase with the height from the basin, with the Red cell showing a small mismatch in this increase when the topmost Brown cell is considered due to the fact that it was partially submerged and partially in air during the tests. The standard deviations of the tests indicate individual tests may not be representative for a good estimate for monitoring and consequently the use of a larger number of tests is recommended to obtain a consistent marker for monitoring that is representative of the location of the sensors, while retaining the fundamental characteristic of what the system is undergoing.

Figure 4 presents the estimated Hurst exponent average values for the five different set-ups considered in this paper. It is observed that the submerged load cell at the bottom (Yellow) is the most representative in tracking the different set-ups considered, giving rise to different types of dynamic responses. While the other submerged cell closer to the free water level is almost constant or only slightly sensitive to such changes, the ones in air are not representative of these changes. Consequently, the location of instrumentation is quite important for tracking changes in structures or

monitoring them. On the other hand, the average and consistent values of estimated Hurst exponents at different locations of sensors and for different set-ups may be representative of the device itself.

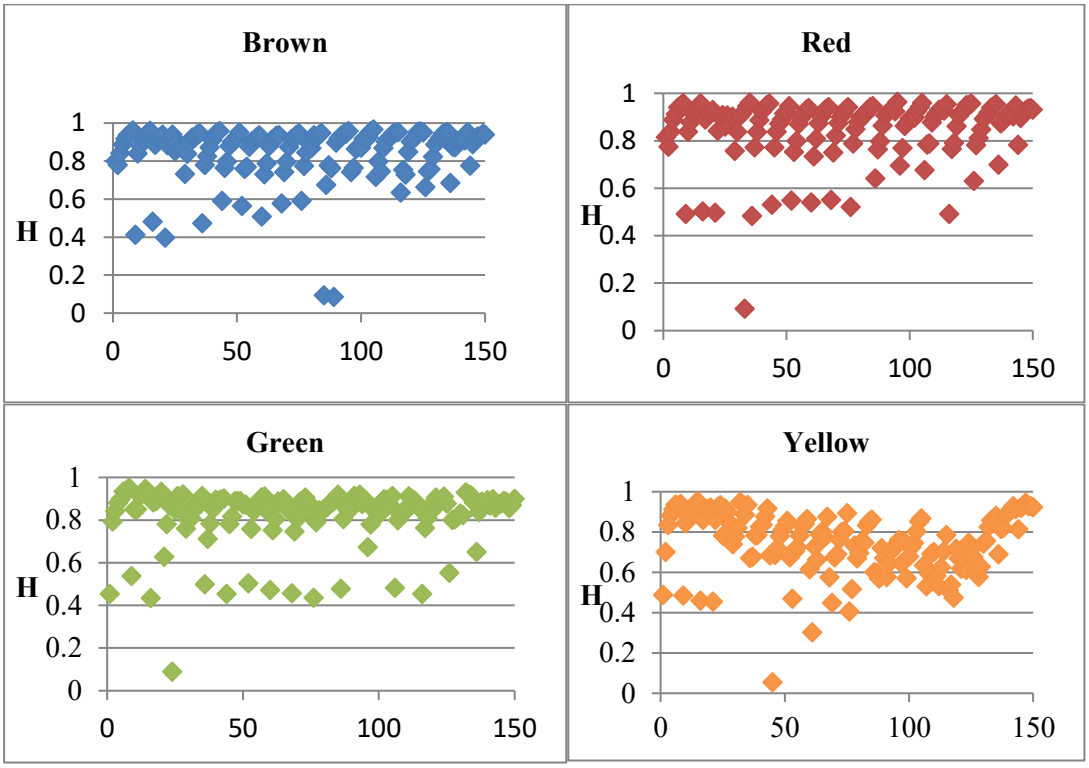

Figure 3. Estimated Hurst exponents for different locations of load cells for a range of experiments.

Table 4. Estimated Hurst exponents for different load cells excluding stillwater values.

	Brown	Red	Green	Yellow
Mean	0.877	0.884	0.859	0.768
Standard Deviation	0.116	0.089	0.089	0.143

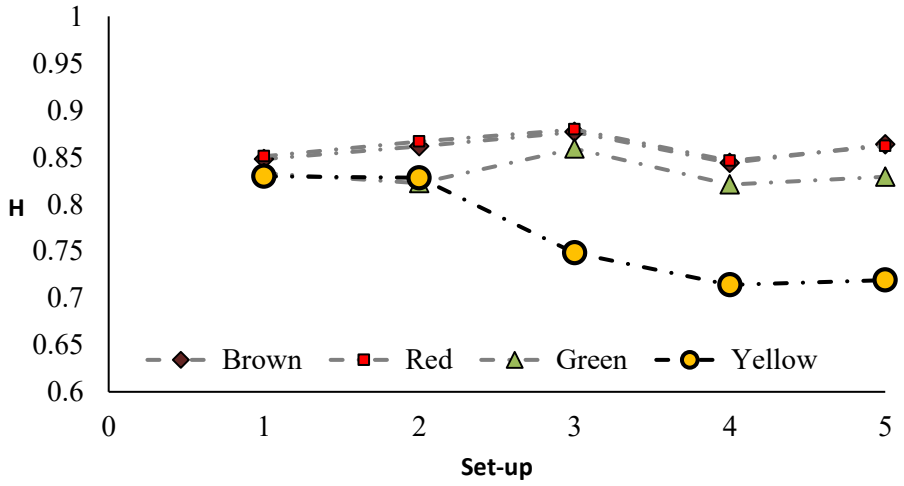

Figure 4. Estimated average Hurst exponents for set-up during experimentation.

5. Discussion and Conclusions

This paper has experimentally presented the potential of Hurst exponent as a possible output-only marker for offshore renewable energy devices. Tests have been carried out in an ocean wave basin and a number of different set-ups have been considered for a Froude scaled monopile model. It is observed that Hurst exponent can be an effective marker for monitoring such devices or platforms when an output from the device is available. In the current paper, the action of waves and equivalent wind forces have been considered at different locations of load cells and it appears that the location of the cell most representative of different loads from water waves is the appropriate location for estimating Hurst exponents. The average estimation of Hurst exponents may be related to the signature of the device itself. Additionally, for the method to be effective, average values over a relatively large number of tests should be carried out.

Previous studies [17, 18] have already shown that such devices typically exhibit nonlinear behaviour although a calibrated theoretical model is not always available. However, estimation of nonlinearity using the structure as a filter is not a new concept [19] and this approach may be extended to the problem under consideration. The requirement of carrying out a relatively larger number of tests is not ideal for rapid assessments, but is often considered as a part of best practice guidelines in normative documents [20]. However, the experiments are usually carried out at a relatively larger scale but in a laboratory environment and consequently it may not be extremely difficult to carry them out. For full-scale deployment, an initial time should be spent to calibrate and benchmark the monitoring markers for any of such structure when the responses are available from a sensor or sensors as a time series. Finally, to obtain better confidence on whether the average values of the estimated Hurst exponents are representative of the signature of the device or not, detailed experiments should be carried out in a wave basin with other offshore renewable energy device solutions. The development of a repository of such device testing can be extremely helpful in this regard.

References

[1] Kaldellis K, Kavadias K and Christinakis E. (2001). Evaluation of the Wind–Hydro Energy Solution for Remote Islands. *Energy Conversion and Management*, vol 9(42) pp. 1105-20.

[2] Lakkoju V. (1996). Combined Power Generation with Wind and Ocean Waves. *Renewable Energy,* vol 9(42) pp. 870-74.

[3] de Vries W and Krolis V. (2007). *Effects of Deep Water on Monopile Support Structures for Offshore Wind Turbines*. EWEC, Milan, 2007.

[4] Agarwal P and Manuel L. (2009). Simulation of Offshore Wind Turbine Response for Long-Term Extreme Load Prediction. *Engineering Structures*, vol 3, pp. 2236-2246.

[5] Standard: Design of Offshore Wind Turbines. (2007). Federal Maritime and Hydrographic Agency.

[6] Swartz RA, Lynch JP, Zerbst S, Sweetman B and Rolfes R. (2010). Structural Monitoring of Wind Turbines using Wireless Sensor Networks. *Smart Structures and Systems*, vol 6(3), pp. 1-14.

[7] Pakzad SN, Fenves GL, Kim S and Culler DE. (2008). Design and Implementation of Scalable Wireless Sensor Network for Structural Monitoring. *ASCE Journal of Infrastructure Systems*. Vol. 14(1), pp. 89-101.

[8] Pakrashi V, Harkin J, Kelly J, Farrell A and Nanukuttan S. (2013). Monitoring and Repair of an Impact Damaged Prestressed Concrete Bridge. *Proceedings of the Institute of Civil Engineers, Journal of Bridge Engineering*, vol. 166(1), pp. 16-29.

[9] Parloo E, Vanlanduit S, Guillaume P and Verboven P. (2004). Increased reliability of reference-based damage identification techniques by usingoutput-only data. *Journal of Sound and Vibration*, vol. 270, pp. 813–832

[10] Pakrashi V, Basu B and O' Connor A. (2009). A Statistical Measure for Wavelet Based

Singularity Detection. *ASME Journal of Vibrations and Acoustics*, vol., 131(4), pp. 041015-1 – 041015-6.

[11] Pakrashi V, O'Sullivan K, O'Shea R and Murphy J. (2013). *Experimental Responses of a Monopile Foundation with a Wave Energy Converter Attached*, Proceedings of the Hydro 2013 International, Chennai, India.

[12] Di Matteo T, Aste T and Dacorogna MM. (2003). Scaling behaviour in differently developed market. *Physica A*, vol. 324, pp. 183 – 188.

[13] Ihlen EAF. (2012). Introduction to multifractal detrended fluctuation analysis in Matlab. *Frontiers in Physiology*, vol. 3(141), pp.1-18.

[14] Pakrashi V, Kelly J, Harkin J and Farrell A. (2013). Hurst Exponent Footprints from Activities on a Large Structural System. *Physica A*, vol. 392(8), pp. 1803 – 1817.

[15] Melhem H and Kim H. (2003). Damage Detection in Concrete by Fourier and Wavelet analyses. *ASCE Journal of Engineering Mechanics*, vol. 129(5), pp. 571-577.

[16] Pakrashi V, Basu B and O' Connor A. (2007). Structural Damage Detection and Calibration using Wavelet-Kurtosis Technique. *Engineering Structures*, vol. 29(9), pp. 2097- 2108.

[17] Murphy J, O'Shea R, O'Sullivan K and Pakrashi V. (2013). Dynamic Responses of a Scaled Tension Leg Platform, Wind Turbine Support Structure in a Wave Tank. *Key Engineering Materials*, vol., 569-570, pp. 563-570,

[18] Jaksic V, O'Shea R, Cahill P, Murphy J, Mandic DP and Pakrashi V. (2015). Dynamic Response Signatures of a Scaled Model Platform for Floating Wind Turbines in an Ocean Wave Basin. *Philosophical Transactions of the Royal Society A: Mathematical, Physical and Engineering Sciences*, vol. 373, pp. 20140078:1-18.

[19] Nichols JM, Todd MD, Seaver M and Virgin LN. (2003). Use of chaotic excitation and attractor property analysis in structural health monitoring. *Physical Review E,* vol. 67, pp. 016209:1-8.

[20] BS 6349-7, Part 7, Design and Construction of Breakwaters.